NASA/TM—2006–214302

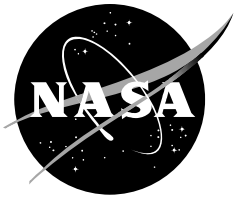

Potential Polymeric Sphere Construction Materials for a Spacecraft Electrostatic Shield

Joseph G. Smith, Jr.
Langley Research Center, Hampton, Virginia

Trent Smith, Martha Williams, and Robert Youngquist
Kennedy Space Center, Florida

Wendell Mendell
Johnson Space Center, Houston, Texas

April 2006

NASA STI Program ... in Profile

Since its founding, NASA has been dedicated to the advancement of aeronautics and space science. The NASA scientific and technical information (STI) program plays a key part in helping NASA maintain this important role.

The NASA STI program operates under the auspices of the Agency Chief Information Officer. It collects, organizes, provides for archiving, and disseminates NASA's STI. The NASA STI program provides access to the NASA Aeronautics and Space Database and its public interface, the NASA Technical Report Server, thus providing one of the largest collections of aeronautical and space science STI in the world. Results are published in both non-NASA channels and by NASA in the NASA STI Report Series, which includes the following report types:

- TECHNICAL PUBLICATION. Reports of completed research or a major significant phase of research that present the results of NASA Programs and include extensive data or theoretical analysis. Includes compilations of significant scientific and technical data and information deemed to be of continuing reference value. NASA counterpart of peer-reviewed formal professional papers but has less stringent limitations on manuscript length and extent of graphic presentations.

- TECHNICAL MEMORANDUM. Scientific and technical findings that are preliminary or of specialized interest, e.g., quick release reports, working papers, and bibliographies that contain minimal annotation. Does not contain extensive analysis.

- CONTRACTOR REPORT. Scientific and technical findings by NASA-sponsored contractors and grantees.

- CONFERENCE PUBLICATION. Collected papers from scientific and technical conferences, symposia, seminars, or other meetings sponsored or co-sponsored by NASA.

- SPECIAL PUBLICATION. Scientific, technical, or historical information from NASA programs, projects, and missions, often concerned with subjects having substantial public interest.

- TECHNICAL TRANSLATION. English-language translations of foreign scientific and technical material pertinent to NASA's mission.

Specialized services also include creating custom thesauri, building customized databases, and organizing and publishing research results.

For more information about the NASA STI program, see the following:

- Access the NASA STI program home page at *http://www.sti.nasa.gov*

- E-mail your question via the Internet to help@sti.nasa.gov

- Fax your question to the NASA STI Help Desk at (301) 621-0134

- Phone the NASA STI Help Desk at (301) 621-0390

- Write to:
  NASA STI Help Desk
  NASA Center for AeroSpace Information
  7121 Standard Drive
  Hanover, MD 21076-1320

NASA/TM—2006–214302

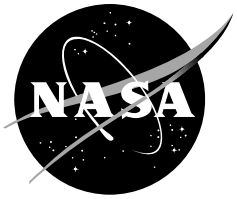

Potential Polymeric Sphere Construction Materials for a Spacecraft Electrostatic Shield

Joseph G. Smith, Jr.
Langley Research Center, Hampton, Virginia

Trent Smith, Martha Williams, and Robert Youngquist
Kennedy Space Center, Florida

Wendell Mendell
Johnson Space Center, Houston, Texas

National Aeronautics and
Space Administration

Langley Research Center
Hampton, VA 23681

April 2006

Available from:

NASA Center for AeroSpace Information
7121 Standard Drive
Hanover, MD 21076-1320
(301) 621-0390

This report is also available in electronic form at

http://ntrs.nasa.gov

POTENTIAL POLYMERIC SPHERE CONSTRUCTION MATERIALS FOR A SPACECRAFT ELECTROSTATIC SHIELD

ABSTRACT

An electrostatic shielding concept for spacecraft radiation protection under NASA's Exploration Systems Research and Technology Program was evaluated for its effectiveness and feasibility. The proposed shield design is reminiscent of a classic quadrupole with positively and negatively charged spheres surrounding the spacecraft. The project addressed materials, shield configuration, power supply, and compared its effectiveness to that of a passive shield. The report herein concerns the identification of commercially available materials that could be used in sphere fabrication. It was found that several materials were needed to potentially construct the spheres for an electrostatic shield operating at 300 MV.

INTRODUCTION

In January 2004, President Bush announced the Vision for Space Exploration describing NASA space policy for the future (1). Two major goals of this Vision were 1) return manned flights to the Moon and 2) an eventual manned landing on Mars. To implement these goals, a new Crew Exploration Vehicle (CEV) and associated technologies have to be developed. The development of these technologies was to be performed under the NASA Exploration Systems Human and Robotic Technology (H&RT) Program [later renamed the Exploration Systems Research and Technology (ESR&T) Program].

One crucial technology in CEV development is Radiation Protection. For a manned Mars mission, astronauts could potentially be exposed to 2 years of radiation (2). Results from the Martian Radiation Environment Experiment (MARIE) on Mars Odyssey measured radiation levels both in Mars transit (April to August 2001) and in low Martian orbit (3,4). In Martian orbit, the radiation levels present were found to be ~2.5 times that present on the International Space Station. These measurements along with others on charge distribution (4) provided confidence in predicting the radiation levels that would be experienced on a trip to Mars.

It is presumed that after launch, the CEV would remain in Earth orbit for some finite period of time for systems checkout before continuing on its mission. The radiation environment present here depends on vehicle location (7). In low Earth orbit (LEO), the radiation environment experienced by the vehicle can vary with orbital inclination. For example, an orbital inclination of <30° would have protons of <100 MeV as the major constituent. Additionally, galactic cosmic radiation (GCR) is assumed to have energies <15 GeV that would peak at 1 GeV. At 90° inclination, solar flare protons of 7 GeV with a majority at <0.5 GeV are prevalent. Electrons are reported to be present at a higher density compared to an orbital inclination of <30°.

Passive and active approaches have been proposed for radiation protection of the vehicle (2,3,5-8). The passive approach is based on materials that possess sufficiently high hydrogen content (i.e water, polyethylene) to absorb radiation. Polyethylene was chosen based on its low mass number (carbon and hydrogen), which minimizes neutron and other secondary particle production (9). Due to its low density (0.9 g/cm^2), a large volume of material is needed to achieve an effective density of 4.8 g/cm^2. At this density, a 22% reduction in radiation to the crew quarters can be realized. The main drawback of the passive shield is that of weight. In the case of polyethylene, flammability is also an issue. Even though there are problems with the passive approach, it is the one currently employed. For example, polyethylene blocks are used on the International Space Station in certain areas for crew radiation protection. Proposed active approaches are based on electromagnetic fields generated by either magnetostatic or electrostatic means and require vehicle power to operate (7a).

In response to an Intramural Call for Proposals in June 2004 by the H&RT Program, the Applied Physics Lab at the Kennedy Space Center (KSC) submitted a proposal entitled "Spacecraft Electrostatic Shielding – Protection, Propulsion, and Energy Delivery (SES) Project". The SES project was an active

radiation shielding approach based on the Electrostatic Shielding Concept (ESC) (5). This project was a basic technology research and development effort conceived by KSC that addressed four H&RT Program system challenges as defined in the Program Formulation Plan. These were:

- **Margins and Redundancy:** The technologies addressed may provide lower mass alternatives to existing radiation shielding, propulsion, and energy supply technologies.
- **ASARA Human Presence in Deep Space**: The concepts may provide enhanced radiation shielding compared to passive shielding and may significantly reduce trip duration by providing continuous propulsion, thereby reducing both exposure levels and durations.
- **Energy Rich Systems and Missions:** The beamed energy acquisition concept may provide an alternative method of generating on-board energy, possibly enabling a more energy-rich system.
- **Reconfigurability:** At the heart of the three concepts being explored is the idea of placing an electrostatic charge around a spacecraft that, once in place, can be used for radiation shielding and/or propulsion and/or energy acquisition depending on the mission phase.

One of the project objectives was to evaluate and determine the viability of creating an electrostatic field around the spacecraft to repel charged particles using a modified electrode configuration. To achieve the objective, the project was divided into two phases with the first evaluating critical technologies such as materials to be used to fabricate the system and power supply feasibility. The second phase was a concept demonstration involving analytical and experimental testing. Project funding was awarded in early FY05 under the Advanced Studies, Concepts, and Tools element of the Advanced Space Technology Program within the H&RT Program. However, the project was terminated in early FY06 due to extensive H&RT program modifications by NASA Headquarters. The work reported herein briefly discusses previous ESC studies conducted over the last 45 years, the KSC ESC, and identification of commercially available materials for the KSC ESC.

THE ELECTROSTATIC SHIELDING CONCEPT

The ESC is based on the principle that like charges repel one another (6-8). For the simplified case, the spacecraft would possess a positive potential to repel protons. However this configuration would attract low energy free electrons toward the vehicle eventually resulting in shield discharge. Additionally, these low energy electrons would impact the vehicle with high kinetic energies resulting in the production of dangerous levels of secondary radiation (bremsstrahlung). Prevention of bremsstrahlung occurrence would require the shield to have a high-energy particle accelerator to remove the accumulated negative charge, which is inherently complicated.

Alternatively, the electrostatic shield could consist of a negative potential surrounding the vehicle that is itself held at a positive potential. This was proposed to be in the form of concentric spheres. Three separate studies were conducted based on this configuration. The first study in 1964 dealt with a two concentric sphere arrangement where the spheres were maintained at equal but opposing charges (6). The second study in 1984 kept the two concentric sphere arrangement but held the outer sphere at a slightly higher negative potential resulting in a net negative charge to the system (7). The third study in 1985 added a third concentric sphere/grid to the structure and maintained this at a slight positive charge (8). Each of these studies is briefly summarized; however, for a more detailed discussion on each of these approaches the reader is directed to the appropriate reference(s).

Spheres of Equal but Opposing Charge (6)

This study focused on two charged concentric spheres where the outer sphere was to be negatively charged while the inner sphere, surrounding the vehicle, was held at a positive potential. The study focused on radiation that was prevalent in the Van Allen Radiation Belts and did not consider Galactic Heavy Ions (HZE denoting high Z and energy). This proposed configuration solved the problem previously described since positively charged species would pass through the negatively charged sphere

while being repelled by the positively charged inner sphere. The outer sphere would act as a static shield against free electrons. The penetration of particles into the inner sphere and subsequent entrance into the crew compartment depended on several factors including the electrostatic potential between the individual spheres, the sphere radii, and the particle energy. In this investigation, the sphere potentials were to be generated using a Van De Graff generator. Voltage breakdown studies were conducted using potentials up to 17 MV. Field emissions were calculated not to be a problem, but the spheres could be coated as an added precaution. It was concluded that discharge due to secondary radiation caused by particle bombardment on the electrode surface was not significant.

The total system weight of this configuration was estimated to be as high as 4500 kg and was based on the following structural components: inner and outer spherical electrodes, support rings for the electrodes, and spacers between the electrodes. The material identified for the shield electrodes and support rings were 6061 aluminum alloy and polystyrene for the electrode separators. Polystyrene has an average dielectric strength of 61 kV/mm and thus could withstand potential gradients of 10 kV/mm. An additional 200 kg was estimated for the power supply with a power to weight ratio of 5.5×10^{-2} kW/kg affording 11 kW of power.

Shield effectiveness was defined as the shield weight needed to reduce the total radiation flux by a prescribed quantity. The shielded volume used in this study was a 2 m diameter sphere. The results of this analysis were then compared to a static shield composed of polyethylene. The weight of the polyethylene static shield was to be equivalent to that of the various electrode sizes of the electrostatic shield. Based on these constraints, the electrostatic shield did not perform as well as the static shield for the various electrode sizes. However, it was stated that secondary radiation would be produced through the interaction of protons with the static polyethylene shield and could thus pose a significant safety hazard. Consequently, the static shield would not be as good as the electrostatic shield where this problem did not exist.

It was determined that to maintain this configuration was not practical since any discrepancy in the coincidence between the two charged spheres would result in a net attraction. To improve the shield effectiveness, it was proposed that the system weight would need to be reduced to be equal to or less than that of the passive shield.

Concentric Sphere System with a Slight Negative Charge (7)

A subsequent ESC investigation looked at this concentric sphere approach taking into account HZE of radiobiological interest [in particular ^{56}Fe with energies up to 1.4 GeV/nucleon (energy arbitrarily chosen for analysis)] to shield the vehicle. The ^{56}Fe ion was chosen since it is the heaviest of the common ions in the GCR spectrum. Additionally, it will cause the highest cumulative radiation dose to interplanetary travelers. This study evaluated three configurations: 1) a single positive shield, 2) equal and oppositely charged concentric spheres, and 3) unequal and oppositely charged concentric spheres.

For the single positive shield, it was calculated that to deflect ^{56}Fe required a potential of ~3 GV. This was ~2 orders of magnitude larger than the output of the then state-of-the-art (SOA) Van De Graff generator, which was <30 MV. It was postulated that if the required potential could be achieved, the low energy electrons present in the environment would impact the vehicle with high kinetic energies resulting in the production of dangerous levels of secondary radiation.

The second configuration, where the concentric sphere system was maintained at an equal but opposite charge (6), was revisited in this study. The conclusion reached here was that spheres of equal but opposing charge would not attract electrons, but would not repel them either.

In order for the negative outer sphere to repel electrons, it had to be maintained at a higher charge than the inner positive sphere resulting in an overall negative charge to the structure. The HZE impinging upon this more negatively charged outer sphere would then acquire additional kinetic energy. Consequently, more energy would then be required to repel a particular HZE particle. This potential was greater than what could be generated by the Van De Graff as previously mentioned.

The relative minimum sizes of the spheres and the minimum shell radii needed to prevent vacuum breakdown of the material was determined using elementary electrostatics. The vacuum breakdown used

in these calculations was 30 kV/mm and was comparable to the previous study (6). The required potential needed for HZE deflection was taken as 3.02 GV based on ^{56}Fe. It was determined that the minimum radial size of the inner and outer spheres was 200 and 400 m, respectively. The size was presumed to be that for a minimum mass shield provided that the spheres were fabricated from the same material(s) and were of the same thickness.

Sphere stability was also considered and found to suffer from the same attraction issues as described in reference 6. To maintain a concentric arrangement required a rigid support structure adding system mass. It was put forth that the materials chosen for the support structure would determine the limiting electric-field intensity instead of the vacuum. Other issues were raised regarding personnel access, controls, and propulsion as possible sites for field breakdown. Additionally, a shock hazard to astronauts conducting an extravehicular activity was raised.

The conclusion was that the electrostatic shield was not attractive for radiation shielding based on the required sphere size and the need for a power supply that was ~2 orders of magnitude greater than that available.

Grid System with a Net Zero Charge (8)

The entitled system concept was based on a spherical porous grid structure to generate the electrostatic field. It suggested that the outer negative sphere be surrounded with another sphere/grid that would be positively charged so as to expel accumulating positive ions from the surface of the former. The net charge on this system of three concentric spheres/grids would be zero so as to repel electrons and avoid an ion expulsion mechanism.

The generation of electromagnetic radiation by electrons emitted from the inner positive sphere (adjacent to the crew compartment) was a major concern due to the generation of X-rays. The calculated levels were ~4 times greater than that allowed for radiation workers (5 rem/yr). However, the conclusion reached here was that the dose rate was low at any particular instance in time and was thus acceptable. It was suggested though that the electron emission be reduced.

Three sources of electron emissions were identified: thermionic, photoelectric, and secondary emission. Photoelectric emission was deemed solvable by shielding the system from UV radiation. It was proposed to coat the negative system elements with UV absorbers (i.e. benzophenones, carbon black, etc.) or to shade the system from the sun. An additional benefit provided by the UV absorber on the sphere surface was that higher field strengths could be attained thus allowing higher voltages. It was postulated that the UV absorber could reduce the current drain on the system in LEO as well. The surface temperature of the cathodic sphere was assumed to be <400K (127°C) and was considered less than that needed to induce thermionic emission. Secondary emission due to electron impingement was addressed by minimizing the mass of the outer sphere either through a grid or thin shell structure.

It was determined that the elimination of a large majority of the proton spectrum required a voltage of 100 MV. To maximize the voltage, the radius of the outer sphere had to be greater than or equal to twice that of the inner sphere. Additionally, it was determined that the electric field (in V/m) for solid sheets or grids was four times greater for the outer sphere than the inner sphere. It was calculated that only relatively moderate electric fields were needed to achieve the high voltages necessary to repel HZE if the system was large and the electrode ratio appropriate. Conclusions were that as electrode size increased the current loss and secondary radiation decreased while keeping power drain in check.

For the outer grid, a net negative charge was needed to repel electrons. However, positive ions would need to be repelled from the grid. To alleviate this proton accumulation required the addition of yet another grid that would be maintained at a positive charge. This additional grid would carry sufficient positive charge so as to avoid an ion expulsion mechanism and to maintain the net charge on the entire system at zero. It was proposed that this outermost grid was an extremely fine mesh that would not contribute significantly to secondary emission.

Calculations showed that the maximum pressure on the system and maximum voltage attained was achieved when the outermost sphere was twice the radius of the inner sphere. These sizes were the same as discussed in the 1984 study (7). The maximum field strength used in this study was 14 kV/mm and was

of the same order of magnitude as the previous two studies. The power loss was determined to be relatively low across the outer electrodes in LEO using maximum voltages of ~1MV to repel inner belt electrons.

It was calculated that maximum shield efficiency was attained when the radius of the outer electrode was twice that of the inner electrode or greater. Additionally the efficiency increased with increasing size for a fixed ratio of outer to inner electrode. Consequently, it was shown that the system weight (composed of the grid, support structure, and generator mass) reduced asymptotically with larger radii. To minimize system weight, it was stated to be desirable to have a good portion of the structure in tension and that the grids be concentric. It was proposed that the underlying structure of the electrostatic shield would consist of cables (e.g. quartz fibers) and lightweight tensile members.

In LEO the minimum radius for a 100 and 300 MV shield was determined to be no less than 5 and 15 m, respectively. These were based on LEO applications for minimum insulator length in order to prevent dielectric breakdown. In high EO (HEO), it was presumed that this would not be the case. Consequently the radii could be smaller (hence the system mass reduced). Shield mass was estimated to be reduced by an additional 20% and was attributed to the reduction in generator mass, which was substantial in LEO. The shield mass for a 300 MV system in HEO was stated to be comparable to that of the 100 MV shield in LEO. It was concluded, based on an optimized electrostatic shield, that it exhibited a performance that was several orders of magnitude better than a passive shield. For a 40 m radius, 300 MV shield in LEO the mass was estimated to be ~5 kg/m^2 for the shielded area. A comparable shield of silicon dioxide (moon dust) was estimated to be ~600 kg/m^2. [Note, silicon dioxide is not a suitable comparison for a passive shield around the vehicle. It would be appropriate for an extra-terrestrial landing site.] The estimated total radiation dose rate for both shields was ~9 rem/yr. It was presumed that additional weight savings could be attained by making the vehicle's (HEO and interplanetary type) conductive skin the inner electrode.

In-flight Experiments

In the mid 1970's, two Russian flight experiments evaluated the ESC using a device on-board the Cosmos 605 and 690 satellites. Initial studies were conducted on Cosmos 605 and verified with data obtained from Cosmos 690. One of the experiments addressed current leakage across the electrode gap, which is a major concern for the ESC. This experiment was performed in LEO (221-424 km altitude) and demonstrated that to maintain an electric field intensity of 15 kV/mm the conduction current did not exceed 10^{-7} A/m^2 (10). Additionally, the power requirements did not exceed 10 W for a field intensity operating at 100 kV over a total shield area of 100 m^2. From the Cosmos 690 experiment, the electrostatic shield conduction data obtained was used to refine the power requirement calculations and the size/weight of the electrostatic shield. For a proposed electrostatic shield operating in the Van Allen Radiation belts the maximum power still did not exceed 10 W for a shield size of 1000 m^2 operating at 1 MV (11). Based on these experiments, it was concluded that the electrostatic shield weight could be 20 to 40 times lower than that of a passive system.

KSC ESC QUADRUPOLE MODIFICATION (5)

The SES project is a modification of the ESC evaluated over the last 45 years. The modification involved replacing the outer negative concentric sphere of earlier proposed designs with small negatively charged spheres located at the end of trusses extending from the sides of a positively charged spacecraft (5). This configuration shown in Figure 1 can be thought of as a classic quadrupole with a small net negative charge. The red and green spheres are negative and positive, respectively. The blue sphere is also positive and represents the protected spacecraft area. This configuration was selected due to its symmetry.

To model the fields generated by this quadrupole configuration a FORTRAN code was developed. This code was also used to plot incoming particle trajectories. The following two figures illustrate the typical results obtained using this code for a large number of particles with various velocities and

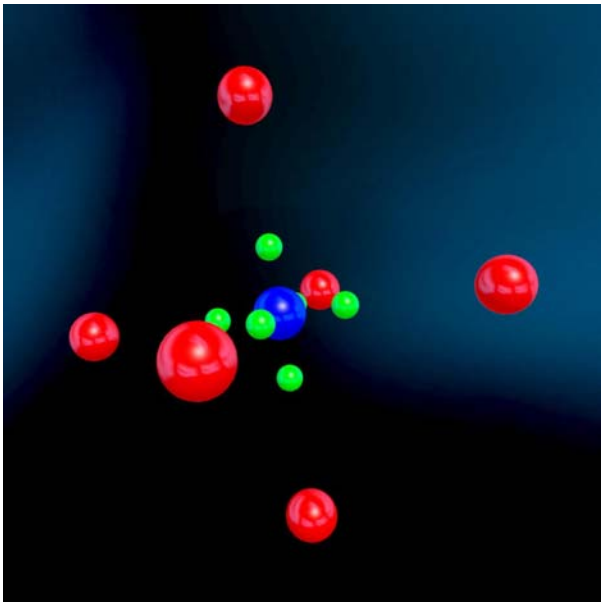

Figure 1: Spacecraft Electrostatic Shield Schematic.

trajectories. The paths taken by positive ions that pass by the negative spheres and are repelled by the positively charged spacecraft are shown in Figure 2, while Figure 3 illustrates the background electrons being repelled by the small net negative charge of the shield. These results imply that for a given voltage, e.g. 100 MV, protons with energies of ≤100 MeV would not reach the spacecraft thus resulting in complete shielding. Protons with energies >100 MeV would be deflected or, if they did impact the spacecraft (e.g. positive sphere), their energy would be reduced by 100 MeV. The latter case would generate less secondary radiation after impact and result in greater effectiveness of a passive shield present on the vehicle than if the particle impacted the passive shield at full energy. The benefits afforded by this configuration were found to scale linearly with shield voltage.

Material composition of the spheres shown in Figure 1 is a serious issue. This is especially true for the negatively charged spheres since UV exposure will supply enough energy to release electrons through the photoelectric effect resulting in sphere discharge. Also at sufficiently high field the electrons can be "pushed" off of the spheres, i.e. vacuum breakdown. One solution to the UV

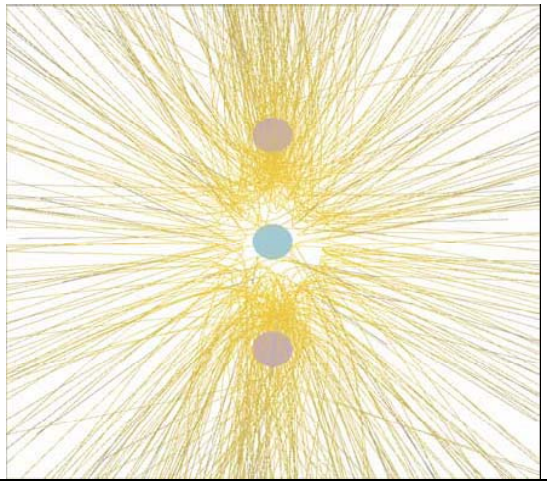

Figure 2: 3D view of positively charged ions being deflected from the spacecraft.

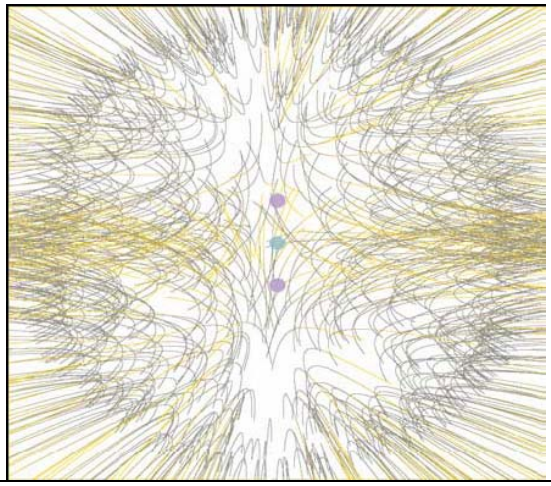

Figure 3: 3D view of electrons being deflected by the negatively charged spheres.

exposure problem would be to coat the negative sphere elements with a UV absorber as suggested in a previous study (8). Potential sphere fabrication materials are to be identified from commercial-off-the shelf (COTS) materials based on material design parameters discussed below. COTS materials were evaluated since the development of an entirely new polymeric material is costly and requires a lengthy development lead-time.

SES Design Parameters

For the SES to be a potential replacement or complement to a passive system, the system would need to be maintained at ≥ 300 MV since much of the GCR is above 1 GeV. A preliminary design shown in Figure 4 and based on the conceptual illustration in Figure 1 is composed of a set of 13 spheres with the

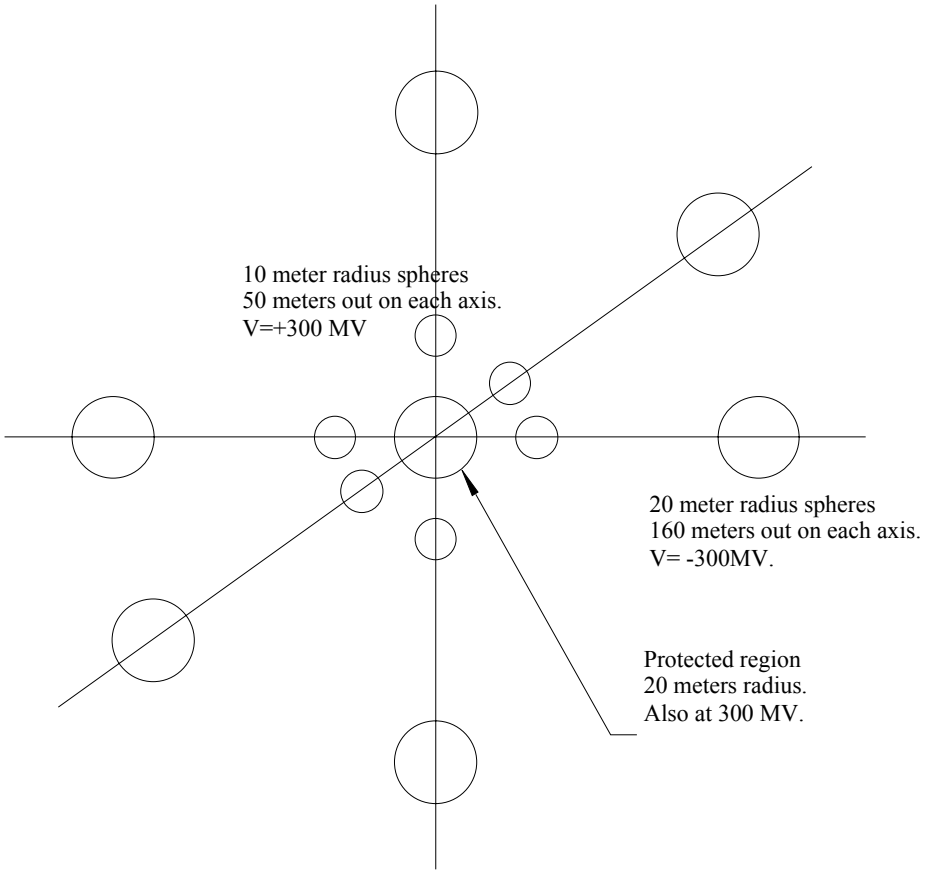

Figure 4: Proposed Spacecraft Electrostatic Shield Design.

center sphere representing the protected region that is the spacecraft itself. The outer spheres are 20 m in radius, located 160 m along each axis, and held at a potential of -300 MV. The inner spheres are 10 m in radius, located 50 meters along each axis, and held at a potential of +300 MV. The outer to inner sphere ratio is 2 and is comparable to that of the previous studies (6-8) albeit at different sizes. These conductive spheres are to be composed of a very thin layer of metal (e.g. gold) deposited on the interior of a polymer film sphere. The polymer to be used in this application has to meet a number of requirements to be used in the space environment. These properties include, but are not limited to, the following:

- Atomic oxygen (AO) resistance (prevalent in LEO)
- Electrical (Dielectric strength, conductivity)
- Mechanical (Tensile strength, crease resistance, etc.)
- Radiation resistance (Gamma, cosmic, galactic, etc.)
- Thermal (Glass transition temperature, coefficient of thermal expansion, etc.)
- UV and VUV resistance

However, many of these requirements cannot be met by any one material. AO resistance is of minor concern for the SES, because the vehicle would reside in LEO for a short time after launch for systems checkout prior to continuing its mission. Due to this short residence time, AO mitigation was not addressed. However, UV exposure is a major concern since the negatively charged spheres would discharge due to UV photons supplying ample energy to the negatively charged sphere surface releasing electrons through the photoelectric effect. For the SES, the most important sphere material properties initially are tensile and dielectric strengths. Prior to potential COTS material identification, the design parameters for these two properties were calculated.

Tensile Strength

The tensile strength of the material to be used in the sphere construction was calculated based on the preliminary design shown in Figure 4. It is related to the tensile pressure (or stress) experienced by the material and is expressed in MPa. The tensile pressure on the sphere is determined by dividing the surface tension, T, by the material thickness. The surface tension on the sphere surface illustrated in Figure 5 is determined from

$$T = \frac{\varepsilon V^2}{2R}$$

where

ε is the permittivity of free space: 8.85×10^{-12} F/m,
V is the potential difference in volts, and
R is the sphere radius in meters.

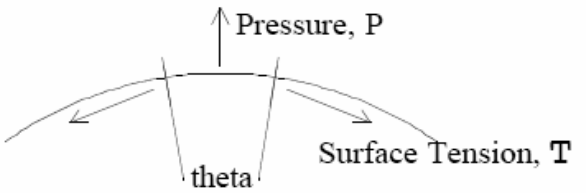

Figure 5: Sphere Surface.

and is expressed in newtons per meter. A full derivation of this formula can be found in Appendix A.

Even though the sphere radii and voltage were identified in Figure 4, it was of interest to assess the effect of a variety of sphere sizes and voltages upon tensile strength. Film thicknesses of 25 and 125 μm were chosen for this evaluation. The calculated tensile strength was subsequently plotted against sphere radii and surface voltages and presented in Figures 6 and 7. The results of this analysis show 1) that for a given sphere radius the tensile strength increased with increasing voltage and 2) that tensile strength decreased with increasing sphere radius at constant voltage regardless of film thickness. The calculated tensile strength was found to decrease for a given sphere radius and voltage with increasing the film thickness from 25 to 125 μm.

As shown in Figure 4, the sphere radii were designated as 10 and 20 m. For these two sphere radii, film thickness was plotted vs. calculated tensile strength and sphere surface voltage (Figures 8 and 9). The results show 1) that for a given film thickness the tensile strength increased with increasing voltage and 2) that tensile strength decreased with increasing film thickness at constant voltage regardless of sphere radius. The highest calculated tensile strengths were obtained for the 25 μm thick film regardless of sphere surface voltage and radius.

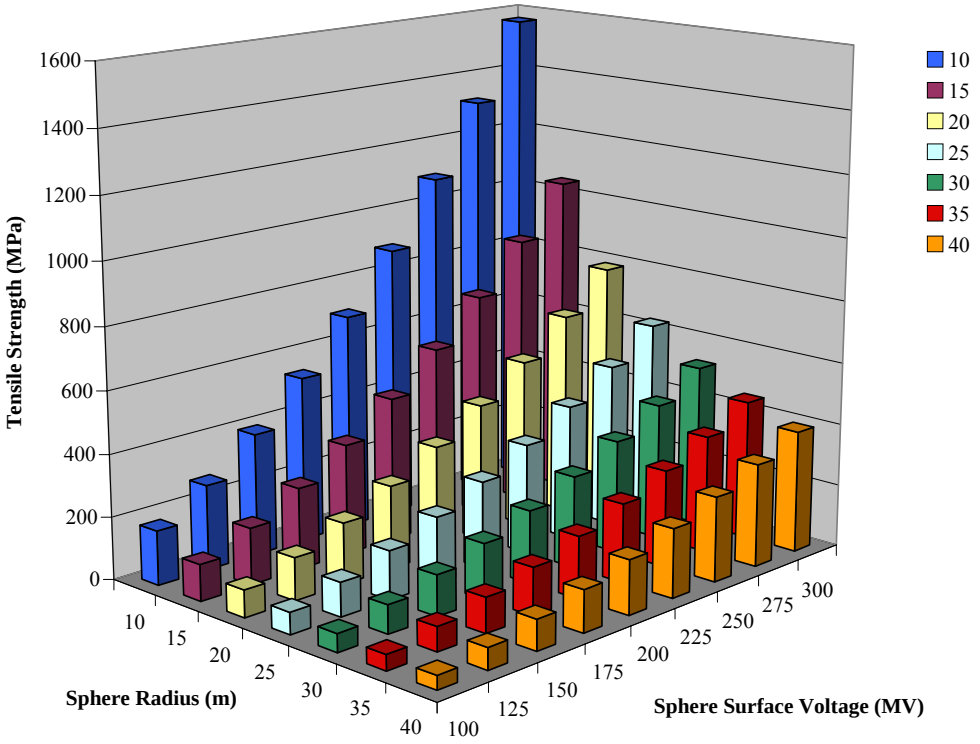

Figure 6: Tensile Strength and Sphere Surface Voltage vs. Sphere Radius for a 25 μm thick film.

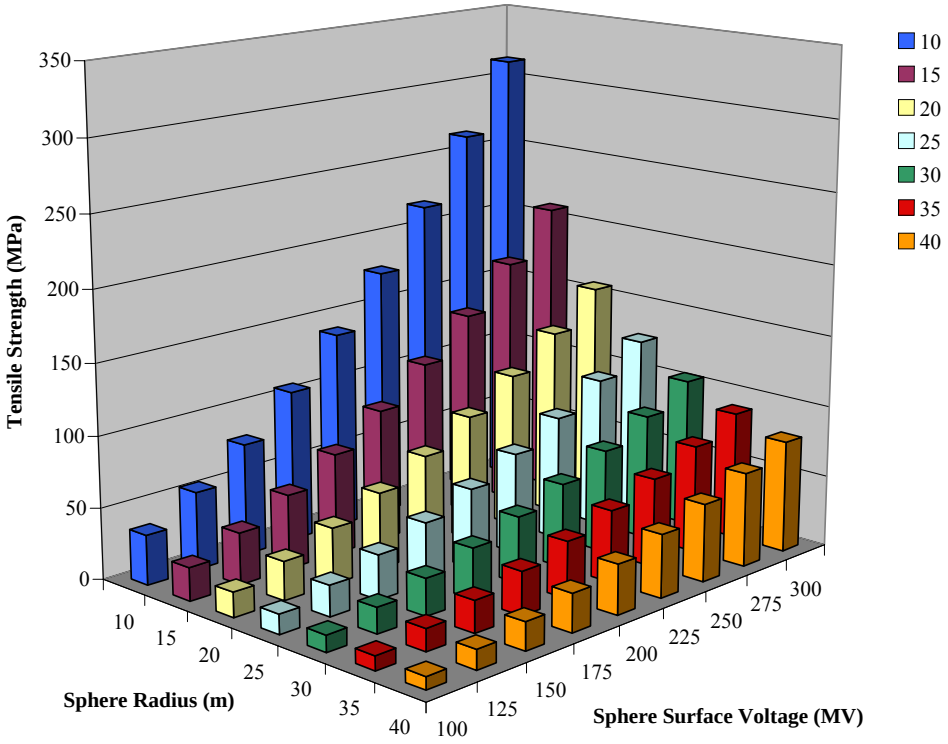

Figure 7: Tensile Strength and Sphere Surface Voltage vs. Sphere Radius for a 125 μm thick film.

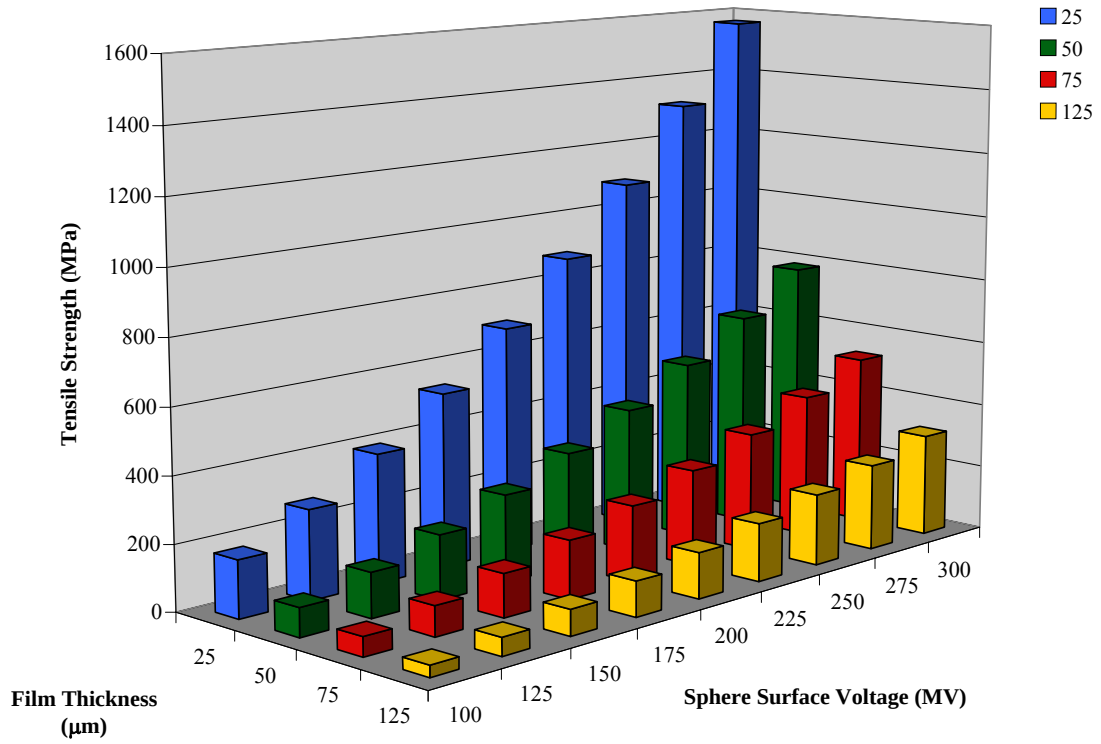

Figure 8: Tensile Strength and Surface Voltage vs. Film Thickness for a 10 m Sphere Radius.

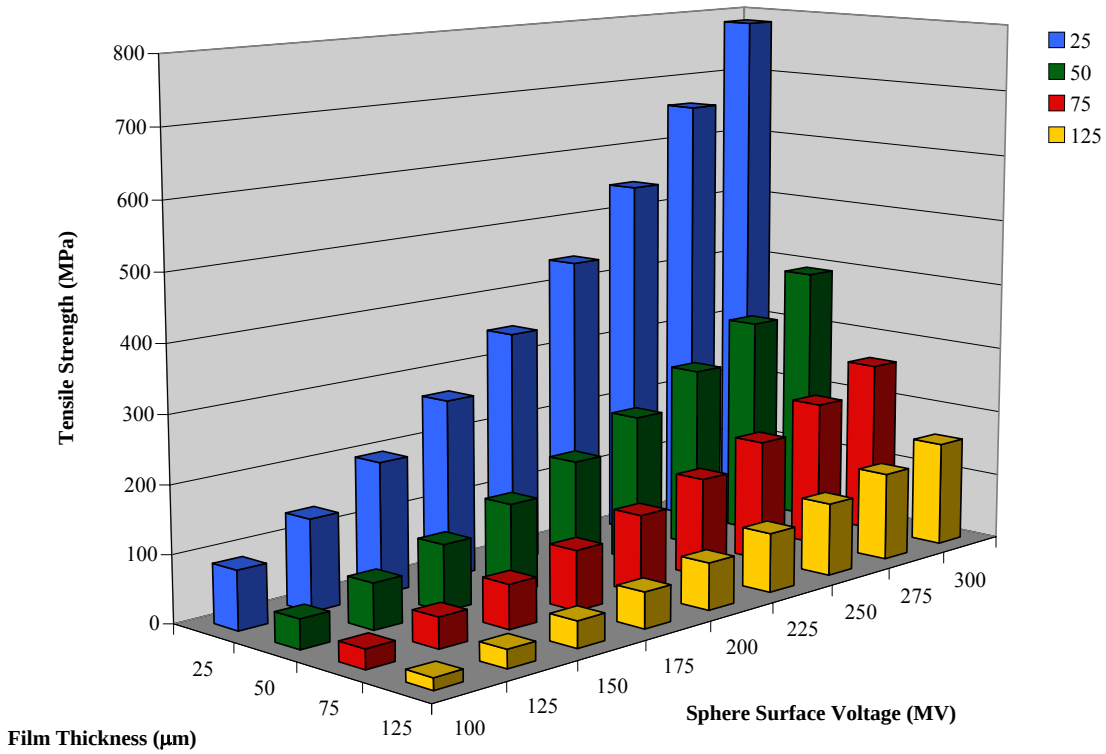

Figure 9: Tensile Strength and Surface Voltage vs. Film Thickness for a 20 m Sphere Radius.

Dielectric Strength

The dielectric strength needed by the material was determined from the electrostatic field ($\vec{E}$) experienced just off the sphere surface shown in Figure 10. $\vec{E}$ is defined as

$$\vec{E} = \frac{V}{R}\hat{r}$$

where

V is the potential difference in volts,
R is the sphere radius in meters, and
$\hat{r}$ is the unit vector

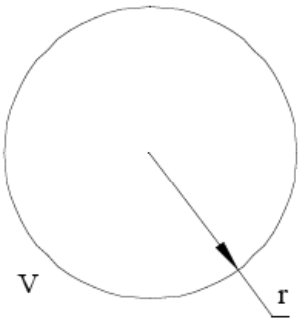

Sphere radius, R, and Voltage, V.

Figure 10: Electrostatic Sphere.

and is expressed in MV/m or kV/mm. For example, a sphere of 10 m radius operating at a voltage of 300 MV would have a $\vec{E}$ of 30 kV/mm. This result is of the same order of magnitude to values used by the previous studies (6-8). It was previously stated though that the electric field experienced by the outer sphere was four times greater than the inner sphere (8). As a result, the required dielectric strength may be as high as 120 kV/mm.

Potential COTS Materials

Aromatic polyimides (e.g. Kapton®), various Teflon® formulations, and polyesters (e.g. Mylar®) have been used in numerous space applications including multilayer insulation blankets, adhesives, threads, collectors, and sunshades/shields. These materials though were not originally designed for the space environment (12). For example, Mylar® exhibits poor radiation and vacuum UV resistance and Teflon® deteriorates when exposed to high-energy radiation. Despite these shortcomings, the materials possessed a desirable combination of properties for the application and, more importantly, were commercially available. Since these materials have been used extensively on spacecraft over the years, they have extensive flight heritage and acceptance in the space community. Other materials (e.g. E, F, H, I from Table 1) have been evaluated for spacecraft applications, but have been under utilized due to lack of flight heritage. LaRC™ CP1 is one example of a relatively new material that has recently been used on a satellite in GEO due to its good thermo-optical properties (13).

Based on the calculated tensile and dielectric strengths determined for the 10 and 20 m sphere radii, several potential COTS materials were identified from these "space qualified" material systems and listed in Table 1. The room temperature DC dielectric and tensile strength properties were obtained from vendor literature. Fiber reinforced materials were not considered because the SES concept is based on ES inflation. Additionally, rigidizable concepts were not considered since the technology relies upon in-situ heating or exposure to the Sun or other light sources to rigidize the structure.

Table 1: Room temperature Tensile and DC Dielectric Strengths

ID	Material	Source	Dielectric Strength, kV/mm	Yield Tensile Strength, MPa	Ultimate Tensile Strength, MPa
A	Kapton® HN	DuPont	303	69	231
B	Kapton® FN[1] (120FN616)		272	61	207
C	Upilex®	UBE	272	206	362
D	Apical®	Kaneka	320	ND[2]	303
E	LaRC™ CP1	SRS Technologies	ND	ND	112
F	LaRC™ CP2		ND	ND	131
G	Ultem™	GE	33	ND	127
H	TOR-LM	Triton Systems, Inc.	127	96	104
I	TOR-NC		190	114	114
J	Mylar®	DuPont Teijin	433	115 (MD) 108 (TD)	216 (MD) 262 (TD)
K	Teflon®	DuPont	18	9	31
L	FEP Teflon®		53	13	23

1. 25 μm thick Kapton® film coated with 2.5 μm thick Teflon® on each side.
2. Not determined.

For the ES to be useful a potential of 300 MV is required. The highest calculated DC dielectric strength was 30 kV/mm for the material to be used as the dielectric layer of the conductive spheres. All materials in Table 1 with the exception of K meet this initial requirement. However the dielectric strength could be as high as 120 kV/mm for the outer sphere based on reference 8. Consequently, materials G and L would be dropped from consideration if this higher dielectric strength were the case. The dielectric strength for E and F are unknown and need to be determined prior to consideration.

The calculated tensile strength needed by the SES configuration in Figure 4 ranged from 157 to 784 MPa for film thicknesses of 125 to 25 μm, respectively, for the 20 m sphere radius at 300 MV (Figure 9). The 20 m sphere requirement is less stringent since it was shown that tensile strength decreased with increasing sphere radius (Figures 6 and 7). The COTS materials in Table 1 able to meet this requirement are the aromatic polyimides A-D and Mylar® (J), but only at a film thickness of 125 μm. But the yield tensile strength of all the materials is lower than the minimum calculated tensile strength of 157 MPa with the exception of material C. Additionally an acceptable margin of safety with respect to the calculated tensile values is not achieved and represents a major problem for SES sphere construction.

One possible solution to this problem is to use a woven fabric surrounding the sphere. This would have an added benefit of allowing the use of a thinner membrane (i.e. 25 μm thick film) that would translate into a mass savings. Liquid crystalline polymers (LCP) such as Kevlar™ and Vectra™ have been used in a number of high performance applications including the airbag fabrics for the recent NASA Mars lander missions – the Spirit and Opportunity robots, as well as Mars Pathfinder that deployed the Sojourner rover. Some of the physical properties of these materials are listed in Table 2.

Table 2: LCP Properties

Property	Vectra™	Kevlar™
Tensile Strength, GPa	3.61	3.20
Tensile Modulus, GPa	83	123
Moisture absorption, %	0	4.3
LCP Type	Thermotropic	Lyotropic

Over the past 5 years work has been performed on the development of a lightweight bumper shield replacement for the Japanese Experiment Module that is to be attached to the International Space Station (14-16). A bumper shield is a covering on a vehicle to prevent catastrophic damage to the vehicle due to high velocity impacts from space debris (natural and man-made) in the 10 to 100 mm size. The current system that is installed on the module is a Whipple bumper shield, but this is thick and heavy. The research resulted in the development of a potential system made out of Vectran™ fibers that are half the areal density and 1/16 the thickness of the currently employed system. Vectran™ was chosen over Kevlar™ due to its low moisture absorption. Absorbed moisture is a concern since the material would outgas once in space. Other desirable properties afforded by Vectran™ include good retention of mechanical properties over a wide temperature range, no discernable creep under simple loads up to 50% of the break strength of a Vectran™ rope, and good radiation resistance. No strength reduction was observed for the material under thermal cycling (30 cycles) from room temperature to 120°C; however, some decrease was observed when the temperature was increased to 195°C.

Vectran™ fabric is of interest to the SES project due to its tensile strength and ability to shield the conductive sphere from damage caused by space debris. This protection is very important because a puncture in the conductive sphere caused by space debris would tear the conductive inner layer resulting in high electric field regions with subsequent breakdown of the polymer and eventual loss of the SES. Thus, this fabric would mitigate both problems by providing tensile strength support and protection from space debris impacts.

UV Mitigation

Exposure of the negatively charged spheres to UV is a concern due to sphere discharge via the photoelectric effect as previously stated. Also, Vectran™ is known to experience a loss in strength when exposed to UV. One solution is to use a UV absorber (i.e. titanium dioxide, zinc oxide, etc.) either as a coating or blending it into Vectran™ or another film (i.e. Kapton®) surrounding the fabric. Coating the material is not desirable, since it can flake off or be damaged resulting in the underlying material being exposed to UV. Blending a UV absorber into Vectran™ at sufficient loading levels to be effective (e.g. 10 wt %) could negatively affect the intrinsic mechanical properties. Consequently a film containing titanium dioxide was chosen to surround the Vectran™ fabric.

The introduction of titanium dioxide into materials as an additive or generated in-situ is known. Titanium dioxide is a photo-responsive material and is best known for its use as a white pigment (17). Kapton® and LaRC™ CP2 were blended with titanium dioxide (R-105A) for use as a protective UV covering. Kapton® was chosen due to its excellent combination of properties and acceptance for use in the space environment. LaRC™ CP2, a low color polyimide, is designed for use in the space environment and has excellent thermo-optical properties that would result in lower thermal loads.

An unoriented Kapton® nanocomposite film was prepared by the addition of titanium dioxide powder to the neat poly(amide acid) with subsequent thermal conversion to the polyimide by heating to 300°C in flowing air for 1 h. Since LaRC™ CP2 is a soluble polyimide, it was solution blended at a comparable loading with titanium dioxide followed by film casting and solvent removal by heating to 250°C in flowing air. These materials were then tested to determine their thermo-optical properties as discussed in the following section.

Sphere Temperature

The sphere thermal profile is important with respect to thermionic emission. In reference 8 it was postulated that this would not be a problem since the sphere surface temperature was assumed to be <400K. For the SES project it was of interest to determine a qualitative sphere thermal profile to see if this was the case. A qualitative sphere thermal profile calculation was performed by NASA JSC using Thermal Desktop/RadCAD and SINDA/FLUINT and presented below.

For discussion of the principles involved, it is convenient to discuss the temperature profile normalized to some convenient maximum temperature relevant to the problem. One such temperature

would be the temperature of a black body in radiative equilibrium (T_{rad}) with the solar constant (at 1 AU, the Earth's distance from the Sun). This is represented as

$$S(1AU) = \sigma(T_{rad})^4$$

where

S(1AU) is 1367 Watts/m^2 and

σ is the Stefan-Boltzmann constant: 5.67 x 10^{-8} W/m^2K^4.

Then T_{rad} = 394K. At the distance of Mars (1.5AU), the equivalent radiative temperature is 322K. If a nonrotating, hollow sphere simply sat in pure radiative equilibrium with the Sun, then the subsolar point would have the temperature T_{rad} and the profile on the sunlit side would reflect the fact that the insolation falls off as the cosine of the polar angle θ (colatitude). The temperature distribution would be constant in the azimuthal direction (longitude) and would be $T_{rad} \cos^{0.25} \theta$ along the surface.

The very thin sphere will at least reradiate across its interior to move heat from the hot to the cold side. Assuming hollow body conduction, the problem becomes one of characterizing the view factors from one element of the interior to any other element. Here every areal element has exactly the same view factor of every other interior element inside a sphere. Thus, every element on the cold side sees about the same heating input; and the cold side of the sphere is almost isothermal. Of course, the temperatures on the hot side are colder than for the case of pure single-surface radiative equilibrium. The temperature distribution is also somewhat evened out by radiative exchange on the hot side of the sphere. Conduction in the skin from the hot pole to the cold one will also level the temperature distribution on the hot side and add a meridional component on the cold side, but it is believed that the effect will be small for the very thin polymer layers.

In this case no conductivity was assumed inside the spherical skin except that the temperature of the outermost-doped polymer layer was identical to that of the inner undoped polymer layer. It was assumed that the gold conductive layer had no effect on the infrared emissivity (and absorptivity) of the inner layer. For temperatures around 200K, the peak blackbody emission wavelength is a few hundred times the thickness of the gold. The photons should barely notice the layer except at glancing angles.

To perform this qualitative analysis, the thermal emissivity (ε) and solar absorptivity (α) for the inner dielectric and outer UV protective layers were determined on lab prepared films. The α pertains to the fraction of incoming solar energy that is absorbed by the film. It was measured on thin films using an AZ Technology Model LPSR-300 spectroreflectometer with measurements taken between 250 to 2800 nm. Vapor-deposited aluminum on Kapton® film (1st surface mirror) was used as the reflective reference for air mass 0 per ASTM E903. The ε is a measure of the films' ability to radiate energy from the film surface and was measured on thin films using an AZ Technology Temp 2000A infrared reflectometer. The thermo-optical properties (α and ε) for Kapton® and LaRC™ CP2 and their corresponding titanium dioxide containing nanocomposites are listed in Table 3. For this analysis LaRC™ CP2 and its titanium doped analog were used for the inner and outer layers due to the materials better thermo-optical properties compared to Kapton®. The better thermo-optical properties of LaRC™ CP2 would result in a lower sphere thermal profile. However, more extensive material characterization of LaRC™ CP2 would need to be performed before using it as a Kapton® replacement.

Table 3: Thermo-optical Properties

Material	Film thickness, μm	α	ε	α/ε
Kapton®	32.5	0.14	0.51	0.28
Kapton® + 10wt% TiO_2	32.5	0.21	0.60	0.35
LaRC™ CP2	70.0	0.07	0.62	0.11
LaRC™ CP2 + 10wt% TiO_2	72.5	0.15	0.67	0.22

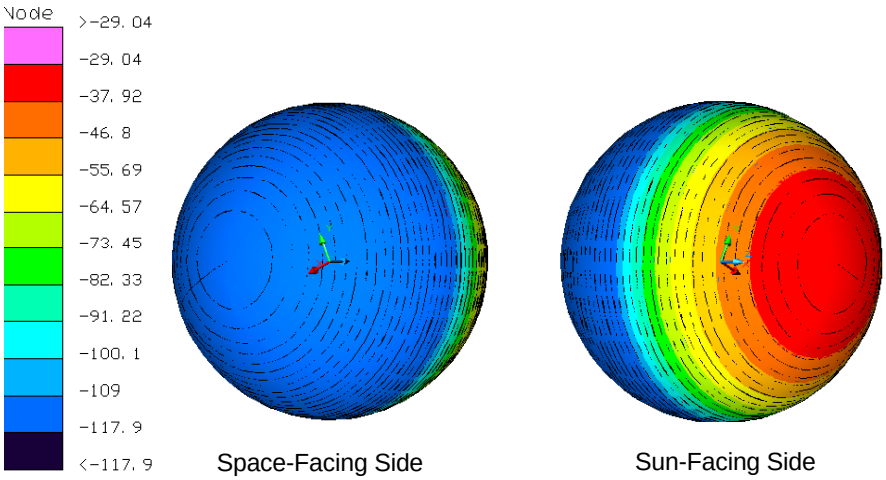

Figure 11: Sphere Surface Steady State Temperatures (°C).

One assumption in generating the sphere thermal profile is that the surface reflectivity and ε is Lambertian. This assumption is required for the view factor calculation to be simple. The qualitative sphere thermal profile is shown in Figure 11. Based on this qualitative analysis it can be seen that thermionic emission would not be a problem as was surmised in reference 8. Since the highest temperature calculated for this profile is approximately -29°C (244K), the use of Kapton® may not be a problem as initially postulated above. However, a more rigorous analysis would need to be performed to verify this is the case.

Sphere Mass

The proposed sphere design is shown in Figure 12. The outer layer would be a 25 μm thick film of Kapton® or LaRC™ CP2 that is filled with titanium dioxide for UV protection of the underlying structure and is represented in green. Vectran™ fabric would handle the sphere tensile load and is represented in blue. It has an areal density of 205 g/cm^2. A 25 μm thick film of Kapton® (in red) with a 65 nm thick gold layer (in gold) represent the inner dielectric and conductive layers, respectively. Based on this proposed construction, the calculated mass for the 10 and 20 m radius spheres is 358 and 1432 kg, respectively. The calculations can be found in Appendix B. Using the proposed SES design in Figure 4 that consists of 6 inner positive spheres (10 m radius) and 6 negative outer spheres (20 m radius), the overall sphere mass of the system is 10,740 kg. This is more than twice that estimated for the system proposed in reference 6, but less than that for the one discussed in reference 8. Additional SES mass would come from the power supply(ies) and associated support structure (e.g. cables, trusses, etc.) holding the spheres in place.

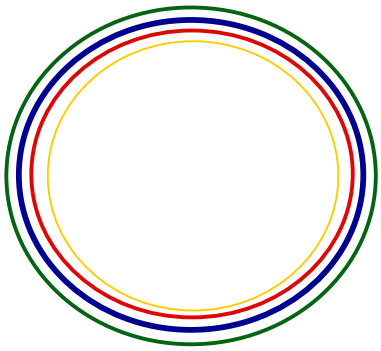

Figure 12: Proposed Sphere Material System Design.

CONCLUSIONS

A potential ES sphere material system has been put forth that addresses problems associated with UV exposure, tensile loads, dielectric strength, and projectile impacts from space debris. The COTS materials are available in sufficient quantities for sphere construction if undertaken. Materials such as Kapton® have extensive space flight heritage and are acceptable candidate materials. Vectran® has been investigated as a potential bumper shield replacement for the Japanese Experimental module and thus has some acceptance. More work on its space environmental durability has to be performed prior to full acceptance. The conductive layer was designated as a vapor-deposited gold coating on Kapton®. Potentially, this inner conductive layer does not have to exhibit the high level of conductivity initially anticipated and thus carbon nanotubes could be used. Research on the use of carbon nanotubes for electrostatic charge dissipation in LaRC™ CP2 and other polymers has been conducted in recent years (18, 19). The use of carbon nanotubes would result in a modest reduction in the designed sphere mass. Based on the current SES construction, the total sphere mass is too heavy for the system to be of practical use relative to a passive shield design. A conceptual design to be evaluated in a future study to address complexity and system mass is based on a torus enveloping the spacecraft as illustrated in Figure 13.

Figure 13: Electrostatic Shield based on a Torus.

The use of trade names or manufacturers does not constitute an official endorsement of such products or manufacturers, either expressed or implied, by the National Aeronautics and Space Administration.

REFERENCES

1. http://www.whitehouse.gov/news/releases/2004/01/20040114-3.html
2. B.L. Ehlmann, J. Chowdhury, T.C. Marzullo, R.E. Collins, J. Litzenberger, S. Ibsen, W.R. Krauser, B. DeKock, M. Hannon, J. Kinnevan, R. Shepard, and F. D. Grant. Acta Astronautica, 56, 851-858 (2005).
3. T.F. Cleghorn, P.B. Saganti, C.J. Zeitlin, and F.A. Cucinotta. Advances in Space Research, 33, 2215-2218 (2004).
4. K.T. Lee, T. Cleghorn, F. Cucinotta, L. Pinsky, and C. Zeitlin. Advances in Space Research, 33, 2211-2214 (2004).
5. P.T. Metzger, J.E. Lane, and R.C. Youngquist. “Asymmetric Electrostatic Radiation Shielding for Spacecraft”, Proc. IEEE Aerospace Conf. (2004) and references therein.
6. F.H. Volger. AIAA Journal, 2(5) 872-878 (1964).
7. a) L.W. Townsend. Physica Medica, XVII, Supplement 1, 84-85 (2001). b) L.W. Townsend. NASA Technical Memorandum 86265. September 1984.
8. W. Frisina. Acta Astronautica, 12, 995-1003 (1985).

9. M.R. Shavers, N. Zapp, R.E. Barber, J.W. Wilson, G. Qualls, L. Toupes, S. Ramsey, V. Vinci, G. Smith, and F.A. Cucinotta. Advances in Space Research, 34, 1333–1337 (2004).
10. E.E. Kovalev and T. Ya. Riabova. Life Sciences and Space Research, 14, 251-253 (1976).
11. E.E. Kovalev and T. Ya. Riabova. Life Sciences and Space Research, 15, 109-111 (1977).
12. C.H.M. Jenkins Ed., Gossamer Spacecraft: Membrane and Inflatable Structures Technology for Space Applications, American Institute of Aeronautics and Astronautics, Inc. 243-254 (2001).
13. http://www.hughespace.com
14. Y. Akahoshi, R. Nakamura, and M. Tanaka. Int. J. Impact Eng, 26, 13-19 (2001).
15. M. Tanaka, Y. Moritaka, Y. Akahoshi, R. Nakamura, A. Yamori, and S. Sasaki. Int. J. Impact Eng, 26, 761-772 (2001).
16. M. Tanaka and Y. Moritaka. Advances in Space Research, 34, 1076-1079 (2004).
17. http://www.titanium.dupont.com
18. J. G. Smith, Jr , J. W. Connell, D. M. Delozier, P. T. Lillehei, K. A. Watson, Y. Lin, B. Zhou and Y. -P. Sun. Polymer, 45, 825-836 (2004) and references therein.
19. K. A. Watson, S. Ghose, D. M. Delozier, J. G. Smith, Jr and J. W. Connell. Polymer, 46, 2076-2085 (2005) and references therein.

Appendix A

Sphere Forces

This document presents a brief derivation of the pressure and surface tension forces on a conducting spherical shell that has been charged to a high voltage. The figures for this document are contained in the document body. Assume that we have a very thin–walled conducting spherical shell of radius, R, and let this shell be raised to a voltage, V, as depicted in Figure 10. If we assume for the moment that the total charge on the shell is given by, Q, then the electrostatic field outside of the shell is given by

$$\vec{E} = \frac{Q}{4\pi\varepsilon_0 r^2}\hat{r}$$

and the corresponding potential (using $\vec{E} = -\nabla\phi$) is given by

$$\phi = -\frac{Q}{4\pi\varepsilon_0 r}$$

Now, using the boundary condition that the potential, ϕ, must equal the applied voltage, V, at r = R, we obtain

$$V = -\frac{Q}{4\pi\varepsilon_0 R}$$

which allows us to write an expression for the total charge in terms of our established parameters, voltage, V, and sphere radius, R,

$$Q = -V\,4\pi\varepsilon_0 R$$

And we can use this to re-express the field in terms of voltage and sphere radius.

$$\vec{E} = -\frac{VR}{r^2}\hat{r}$$

In particular we are interested in the field just off of the surface of the sphere (i.e. when r = R), in which case

$$\vec{E} = -\frac{V}{R}\hat{r}$$

For example, if the sphere is raised to a voltage of 100 MV (million volts) and has a radius of 10 meters then the field at the surface (this would be the field that the polymer sees) is equal to 10 MV/meter, or 10 kV/mm.

We are now in a position to find an expression for the outward directed pressure exerted on the sphere. Start by simply noting that the surface charge density, ρ, is given by

$$\rho = \frac{Q}{4\pi R^2} = -\frac{\varepsilon_0 V}{R}$$

so over an infinitesimal area, dA, we have charge, dQ given by

$$dQ = \rho dA = -\frac{\varepsilon_0 V}{R}dA$$

Now, imagine that this tiny area is lifted just above the surface of the sphere. It will feel a force, $\vec{F}$, equal to the charge times the field at that location,

$$\vec{F} = dQ\vec{E} = \varepsilon_0 \frac{V^2}{R^2} dA\hat{r}$$

obviously directed outward as shown. The pressure, $\vec{P}$, is given by the force per unit area and can be expressed simply as

$$\vec{P} = \frac{\vec{F}}{dA} = \varepsilon_0 \frac{V^2}{R^2} \hat{r}$$

Recalling that $\varepsilon_0 = 8.85 \times 10^{-12}$ F/m, if we had a sphere raised to 100 MV (million volts) and a radius of 10 meters, the outwardly directed pressure would be 885 Pascals. Since there are about 100,000 Pascals in an atmosphere this is only about 1/100th of an atmosphere. But if we raised the potential to 330 MV then the pressure would be ten times higher and would be about 1/10th of an atmosphere.

Now we need an expression for the surface tension, T, which will be in units of force/length. The total ripping force across any given length, l, of material would then be Tl and the tensile pressure (related to Tensile Strength) will be given by T/d, where d is the thickness of the film (T/d is in units of Pascals and is the angular stress aligned along the sphere surface).

Start by choosing our small surface element dA to be a very small round piece of the the sphere surface. We require this small element to be in static equilibrium, by which we mean that all of the forces on it must sum up to zero (see Figure 5). Let the radius of this small piece be a (this variable will drop out) so that the area is given by $dA = \pi a^2$ and the circumference is given by $2\pi a$. Consequently, the total radial component force due to the electrostatic pressure is given by

$$F_P = PdA = \varepsilon_0 \frac{V^2 \pi a^2}{R^2}$$

and this outward force must be matched by the inward projection of the total tensile force, FT , given by

$$F_T = Sin\left(\frac{\vartheta}{2}\right) T\, 2\pi a\,.$$

The angle θ is very small and is equal to 2a/R. Using the small angle approximation for the Sin yields

$$F_T = \frac{2T\pi a^2}{R}$$

Equating these two forces, i.e. setting $F_P = F_T$ yields the final result

$$T = \frac{\varepsilon V^2}{2R}$$

Appendix B

Sphere Mass Calculations

1. Kapton® HN mass with respect to sphere radius and film thickness

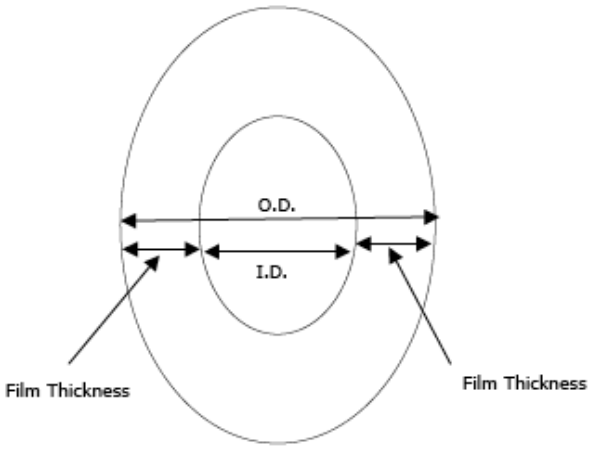

$$\text{sphere volume } (m^3) = \frac{4}{3}\pi * \left(\frac{\text{inner diameter}}{2}\right)^3$$

outer diameter (m) = sphere diameter + 2* film thickness

$$\text{material volume } (m^3) = \frac{4}{3}\pi * \left(\frac{\text{outer diameter}}{2}\right)^3 - \text{sphere volume}$$

$$\text{material mass (g)} = \rho_{Kapton®} * \text{material volume } (cm^3)$$

Film Thickness		Sphere Inner Diameter	Sphere Outer Diameter	Sphere Volume	Material Volume	Material Mass
mil	μm	m	m	m^3	cm^3	kg
1	25	80	80.00005	268083	502655	714
2	50	80	80.00010	268083	1005311	1428
3	75	80	80.00015	268083	1507967	2141
5	125	80	80.00025	268083	2513282	3569
1	25	60	60.00005	113097	282744	401
2	50	60	60.00010	113097	565488	803
3	75	60	60.00015	113097	848232	1204
5	125	60	60.00025	113097	1413723	2007
1	25	40	40.00005	33510	125664	178
2	50	40	40.00010	33510	251328	357
3	75	40	40.00015	33510	376993	535
5	125	40	40.00025	33510	628323	892
1	25	20	20.00005	4189	31416	45
2	50	20	20.00010	4189	62832	89
3	75	20	20.00015	4189	94249	134
5	125	20	20.00025	4189	157082	223

Kapton® HN density = 1.42 g/cm^3

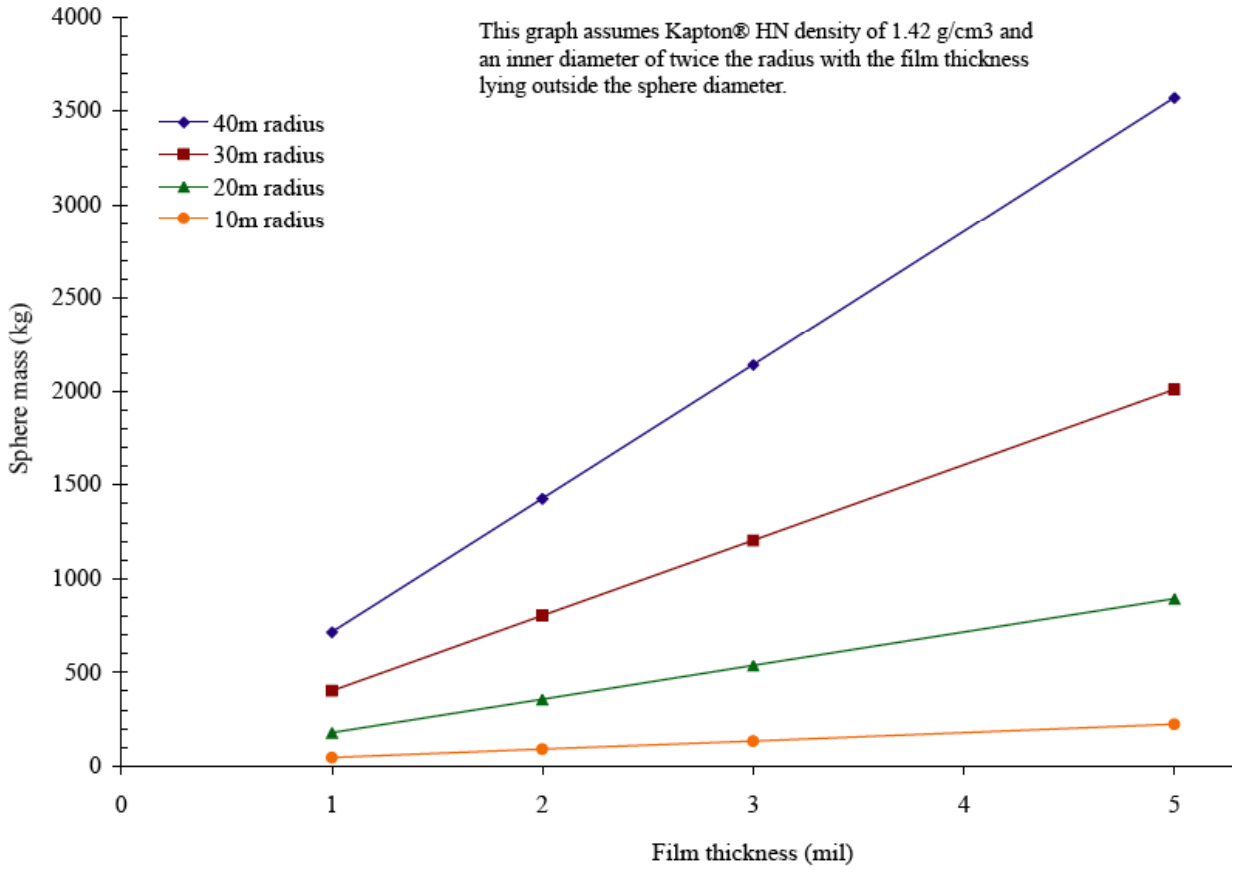

2. Gold (Au) mass with respect to sphere radius and film thickness

$$\text{outer volume } (m^3) = \frac{4}{3}\pi * (\text{sphere radius})^3$$

$$\text{inner volume } (m^3) = \frac{4}{3}\pi * \left[\text{sphere radius} - 2 * \left(\text{Au thickness} * 10^{-9}\right)\right]^3$$

$$\text{material volume } (m^3) = \text{outer volume} - \text{inner volume}$$

$$\text{Au mass (kg)} = \rho_{Au} * (\text{material volume}) * 1000$$

Sphere Radius, m →		10	20	30	40
Thickness, nm	Conductivity, x 10^7 S/m	Gold (Au) mass, kg			
10	1.43	0.485	1.940	4.366	7.761
65	2.87	3.153	12.612	28.376	50.446
150	3.89	7.276	29.104	65.483	116.415
300	4.02	14.552	58.207	130.967	232.830

Gold density = 19.3 g/cm^3 and bulk conductivity = 4.10 x 10^7 S/m

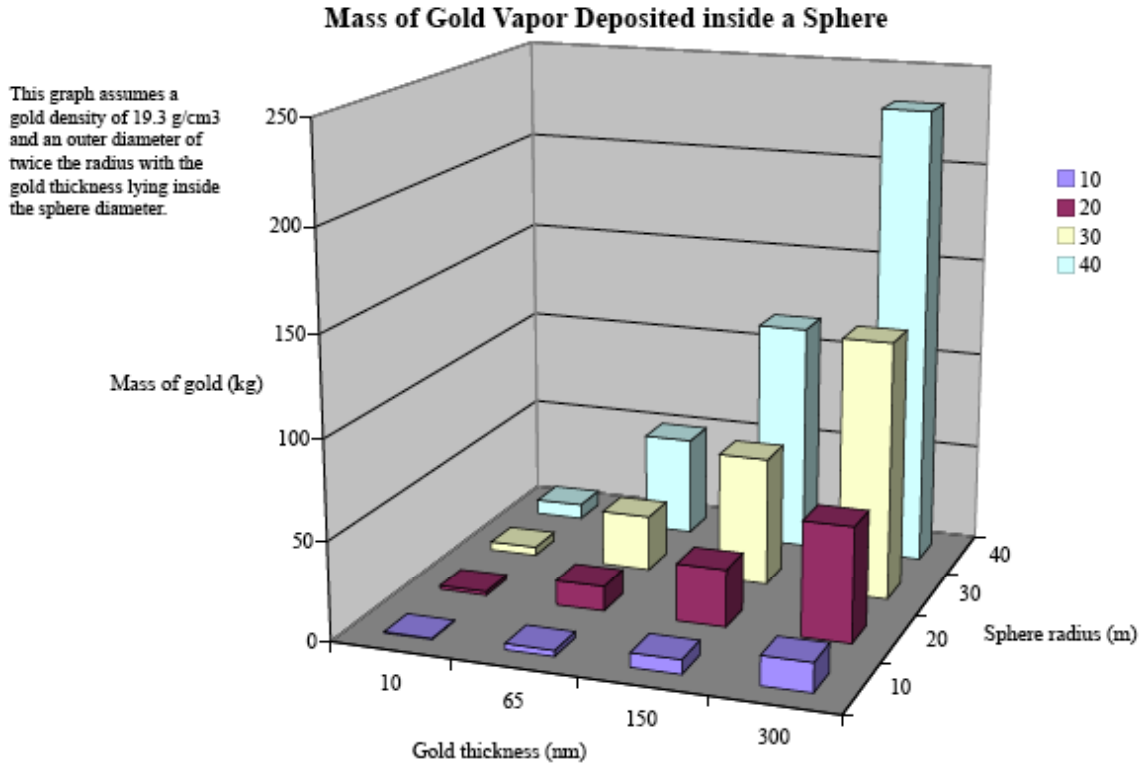

Sphere Radius, m →	10	20	30	40
Outer volume, m^3 →	4188.79021	33510.32164	113097.3355	268082.5731
Gold Thickness, nm	Inner volume, m^3 (material volume x 10^{-4} m^3), [material mass, kg]			
10	4188.79018 (0.251) [0.49]	33510.32154 (1.005) [1.94]	113097.3353 (2.262) [4.37]	268082.5727 (4.021) [7.76]
65	4188.79004 (1.633) [3.15]	33510.32098 (6.535) [12.61]	113097.3341 (14.703) [28.38]	268082.5705 (26.138) [50.45]
150	4188.78983 (3.770) [7.28]	3310.32013 (15.080) [29.10]	113097.3321 (33.929) [65.48]	268082.5671 (60.319) [116.41]
300	4188.78945 (7.540) [14.55]	33510.31862 (30.159) [58.21]	113097.3287 (67.858) [130.97]	268082.5610 (120.637) [232.83]

3. Fabric mass with respect to sphere radius and film thickness

$$\text{sphere area } (m^2) = 4\pi * (\text{sphere radius})^2$$

$$\text{fabric mass (kg)} = \frac{[(\text{sphere area}) * (\text{fabric density})]}{1000}$$

Aramid fabric with an aereal density of 85 g/m2

Sphere Radius, m →	10	20	30	40
Sphere Area, m^2 →	1256.6	5026.5	11309.7	20106.2
Fabric mass, kg →	106.8	427.3	961.3	1709.0

Aramid fabric with an aereal density of 205 g/m2

Sphere Radius, m →	10	20	30	40
Sphere Area, m^2 →	1256.6	5026.5	11309.7	20106.2
Fabric mass, kg →	257.6	1030.4	2318.5	4121.8

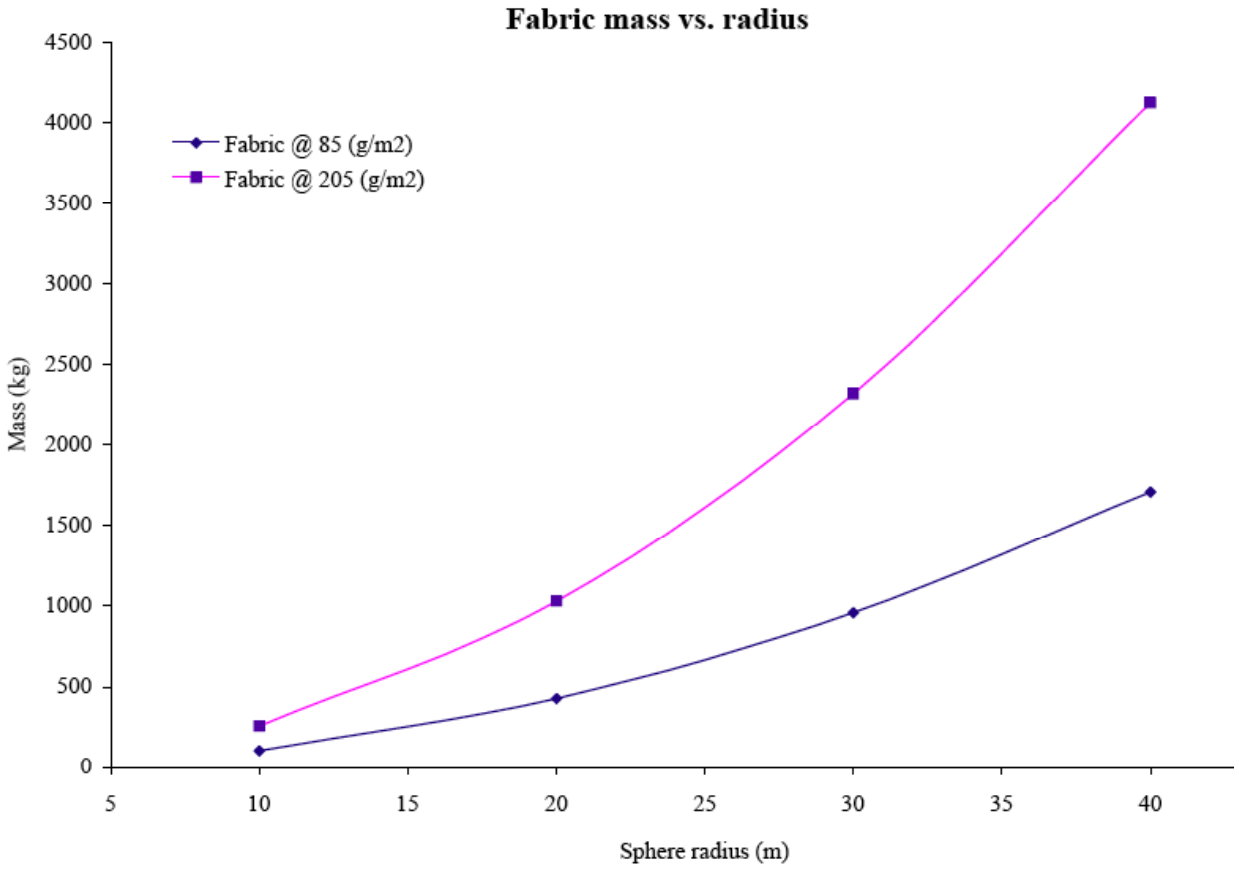

4. (Kapton® HN + 10% TiO_2) mass with respect to sphere radius and film thickness

$$\text{sphere outer diameter (m)} = \text{inner diameter} + 2 * (\text{film thickness})$$

$$\text{calculated density (g/cm}^3) = 0.9\rho_{Kapton® HN} + 0.1\rho_{TiO_2}$$

$$\text{sphere volume (m}^3) = \frac{4}{3}\pi * \left(\frac{\text{inner dimater}}{2}\right)^3$$

$$\text{material volume (cm}^3) = \left[\frac{4}{3}\pi * \left(\frac{\text{outer diameter}}{2}\right)^3 - \text{sphere volume}\right] * 100^3$$

$$\text{material mass (kg)} = \left(\frac{\rho_{film} * \text{material volume}}{1000}\right)$$

Film Thickness		Sphere Inner Diameter	Sphere Outer Diameter	Sphere Volume	Material Volume	Material Mass
mil	μm	m	m	m^3	cm^3	kg
1	25	80	80.00005	268083	502655	843
2	50	80	80.00010	268083	1005311	1687
3	75	80	80.00015	268083	1507967	2530
5	125	80	80.00025	268083	2513282	4217
1	25	60	60.00005	113097	282744	474
2	50	60	60.00010	113097	565488	949
3	75	60	60.00015	113097	848232	1423
5	125	60	60.00025	113097	1413723	2372
1	25	40	40.00005	33510	125664	211
2	50	40	40.00010	33510	251328	422
3	75	40	40.00015	33510	376993	633
5	125	40	40.00025	33510	628323	1054
1	25	20	20.00005	4189	31416	53
2	50	20	20.00010	4189	62832	105
3	75	20	20.00015	4189	94249	158
5	125	20	20.00025	4189	157082	264

*Calculated density = 1.678 g/cm^3; TiO_2 density = 4.0 g/cm^3

5. System mass with respect to sphere radius and film thickness

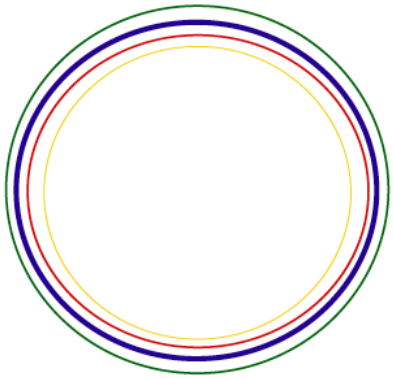

Color	Layer descripton
Gold	Gold
Red	1 mil Kapton®
Blue	Aramid Fabric
green	1 mil Kapton® with UV absorber (10% TiO_2)

$$\text{total mass (kg)} = \text{Gold} + \text{Kapton}^{®}\text{HN} + \text{Fabric} + \left(\text{Kapton}^{®}\text{HN} + \text{TiO}_2\right)$$

Sphere radius, m	1 mil Kapton® & 10% TiO_2, kg	Fabric @ 85 g/cm^2, kg	Gold 65 nm, kg	1mil Kapton®, kg	Total mass, kg
10	52.72	106.81	3.15	44.61	257.61
20	210.86	427.26	12.61	178.44	1030.44
30	474.44	961.33	28.38	401.50	2318.50
40	843.46	1709.03	50.45	713.77	4121.77

Sphere radius, m	1 mil Kapton® & 10% TiO_2, kg	Fabric @ 205 g/cm^2, kg	Gold 65 nm, kg	1mil Kapton®, kg	Total mass, kg
10	52.72	257.6	3.15	44.61	358.08
20	210.86	1030.4	12.61	178.44	1432.31
30	474.44	2318.5	28.38	401.50	3222.82
40	843.46	4121.8	50.45	713.77	5729.48

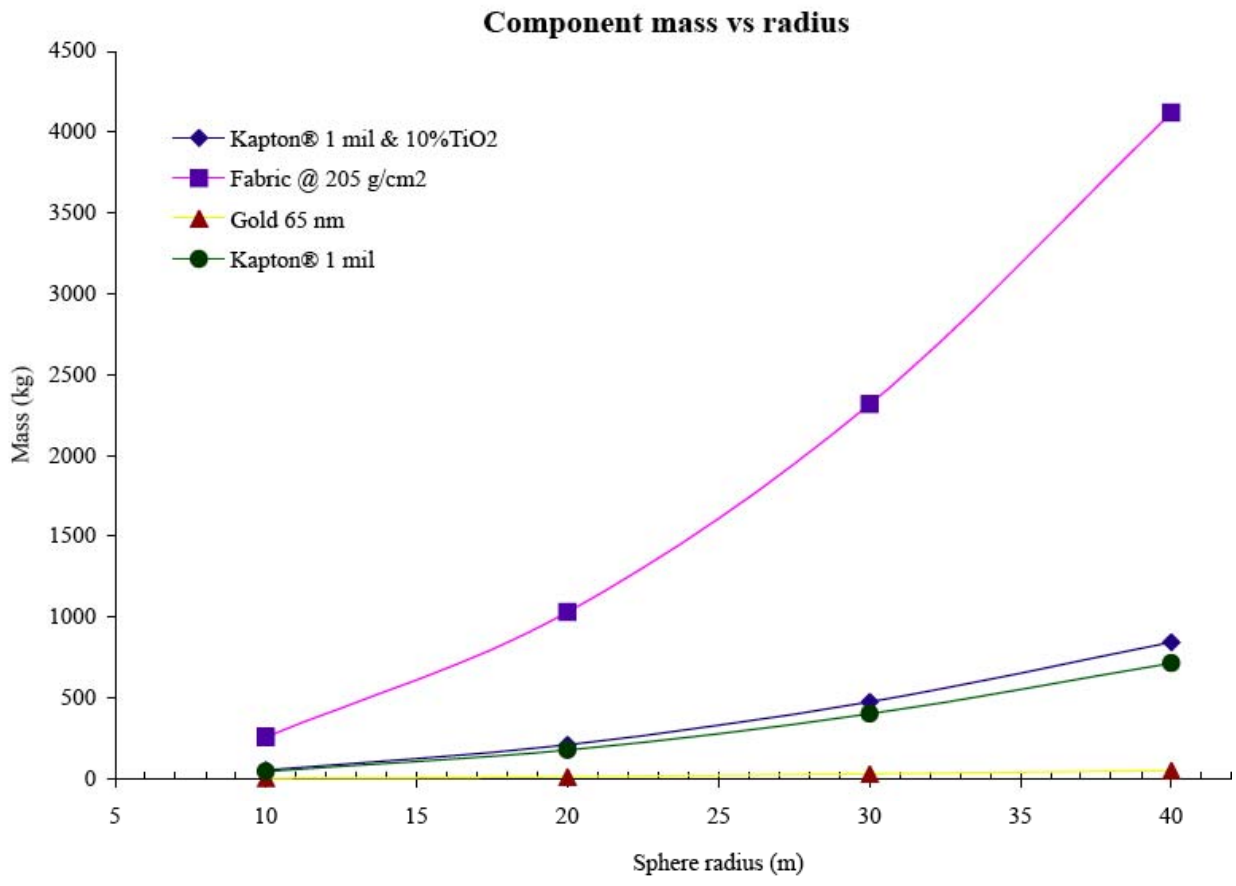

REPORT DOCUMENTATION PAGE

Form Approved
OMB No. 0704-0188

1. REPORT DATE *(DD-MM-YYYY)*	2. REPORT TYPE	3. DATES COVERED *(From - To)*
01- 04 - 2006	Technical Memorandum	

4. TITLE AND SUBTITLE

Potential Polymeric Sphere Construction Materials for a Spacecraft Electrostatic Shield

5a. CONTRACT NUMBER

5b. GRANT NUMBER

5c. PROGRAM ELEMENT NUMBER

6. AUTHOR(S)

Smith, Joseph G.; Smith, Trent; Williams, Martha; Youngquist, Robert; and Mendell, Wendell

5d. PROJECT NUMBER

5e. TASK NUMBER

5f. WORK UNIT NUMBER

612-10-04-23

7. PERFORMING ORGANIZATION NAME(S) AND ADDRESS(ES)

NASA Langley Research Center
Hampton, VA 23681-2199

8. PERFORMING ORGANIZATION REPORT NUMBER

L-19251

9. SPONSORING/MONITORING AGENCY NAME(S) AND ADDRESS(ES)

National Aeronautics and Space Administration
Washington, DC 20546-0001

10. SPONSOR/MONITOR'S ACRONYM(S)

NASA

11. SPONSOR/MONITOR'S REPORT NUMBER(S)

NASA/TM-2006-214302

12. DISTRIBUTION/AVAILABILITY STATEMENT

Unclassified - Unlimited
Subject Category 27
Availability: NASA CASI (301) 621-0390

13. SUPPLEMENTARY NOTES

An electronic version can be found at http://ntrs.nasa.gov

14. ABSTRACT

An electrostatic shielding concept for spacecraft radiation protection under NASA's Exploration Systems Research and Technology Program was evaluated for its effectiveness and feasibility. The proposed shield design is reminiscent of a classic quadrupole with positively and negatively charged spheres surrounding the spacecraft. The project addressed materials, shield configuration, power supply, and compared its effectiveness to that of a passive shield. The report herein concerns the identification of commercially available materials that could be used in sphere fabrication. It was found that several materials were needed to potentially construct the spheres for an electrostatic shield operating at 300 MV.

15. SUBJECT TERMS

Spacecraft radiation protection; Radiation shielding; Polymers; Tensile strength

16. SECURITY CLASSIFICATION OF:			17. LIMITATION OF ABSTRACT	18. NUMBER OF PAGES	19a. NAME OF RESPONSIBLE PERSON
a. REPORT	b. ABSTRACT	c. THIS PAGE			STI Help Desk (email: help@sti.nasa.gov)
U	U	U	UU	31	19b. TELEPHONE NUMBER *(Include area code)* (301) 621-0390